Genome-wide activation screens to increase adeno-associated virus production

Christopher R. Barnes,[1,7] Hyuncheol Lee,[2,7] David S. Ojala,[1] Kazuomori K. Lewis,[3] Prajit Limsirichai,[4] and David V. Schaffer[1,2,3,5,6]

[1]Department of Chemical and Biomolecular Engineering, University of California, Berkeley, Berkeley, CA 94720, USA; [2]California Institute for Quantitative Biosciences (QB3), University of California, Berkeley, Berkeley, CA 94720, USA; [3]Department of Bioengineering, University of California, Berkeley, Berkeley, CA 94720, USA; [4]Department of Plant and Microbial Biology, University of California, Berkeley, Berkeley, CA 94720, USA; [5]Department of Cell and Molecular Biology, University of California, Berkeley, Berkeley, CA 94720, USA; [6]Helen Wills Neuroscience Institute, University of California, Berkeley, Berkeley, CA 94720, USA

We describe a genome-wide screening strategy to identify target genes whose modulation increases the capacity of a cell to produce recombinant adeno-associated viral (AAV) vector. Specifically, a single-guide RNA (sgRNA) library for a CRISPR-based genome-wide transcriptional activation screen was inserted into an AAV vector, and iterative rounds of viral infection and rescue in HEK293 producer cells enabled the enrichment of sgRNAs targeting genes whose upregulation increased AAV production. Numerous gain-of-function targets were identified, including spindle and kinetochore associated complex subunit 2 (SKA2) and inositol 1, 4, 5-trisphosphate receptor interacting protein (ITPRIP). Furthermore, individual or combinatorial modulation of these targets in stable producer cell lines increased vector genomic replication and loading into AAV virions, resulting in up to a 3.8-fold increase in AAV manufacturing capacity. Our study offers an efficient approach to engineer viral vector producer cell lines and enhances our understanding of the roles of SKA2 and ITPRIP in AAV packaging.

INTRODUCTION

Vectors based on the adeno-associated virus (AAV) have been increasingly successful in numerous human gene therapy clinical trials, leading to recent FDA approved products for Leber's congenital amaurosis type 2 and spinal muscular atrophy type 1.[1,2] These two indications involve intraocular administration of a small dose (1.5×10^{11} viral genomes [vg]/eye)[3] or systemic administration of a high dose (1.1×10^{14} vg/kg)[4] to infants, such that these treatments are not burdened by exceedingly high overall manufacturing needs. However, numerous targets currently under development entail systemic administration of larger doses to older and thus larger patients;[5–10] for example, numerous studies have involved administration of $\sim 10^{16}$ vg per patient, which poses a major manufacturing challenge (and in some cases only 1–2 doses per bioreactor run).[11–15] These problems become nearly intractable in manufacturing vector for systemic administration in rare conditions afflicting adult patients and especially in diseases affecting large patient numbers. More efficient, targeted vectors—generated by directed evolution or other vector engineering approaches[16–19]— offer the potential for enhanced efficacy at lower dosages. However,

in general, the field needs substantial improvements in vector production.[11,20]

Just as wild-type (WT) AAV serotypes did not naturally evolve into optimal therapeutic gene delivery vehicles, HEK293 and other vector manufacturing cell lines were not originally created as AAV producer cells, so there is likely considerable room for improvement. The rational design of improved producer lines is challenged by the mechanistic complexity of viral replication and packaging;[21–23] however, again by analogy with capsid evolution, unbiased library-based approaches have the potential to yield improved AAV production systems.

Here, we conduct a genome-wide screen to select for gene targets whose modulation enhances the AAV manufacturing capacity of HEK293T cells. By using Cas9 activation machinery, along with guide RNA libraries within an AAV vector, iterative infection and rescue of producer cells with the vector libraries led to the progressively increased prevalence of guide RNAs targeting genes that increase AAV production. Subsequent clonal analysis of individual guide RNA "hits," along with corresponding cDNA overexpression, yielded up to a 4-fold increase in AAV production. Subsequent mechanistic analysis revealed that overexpression of two key hits increased vector genome replication, as well as the proportion of viral capsids containing a DNA genome (i.e., the full/empty capsid ratio). These results show that this generalizable selection method is capable of identifying genetic targets that increase AAV manufacturing capacity and may yield insights into biological mechanisms of AAV production and packaging.

RESULTS

Selection for guide RNAs that increase AAV titer in HEK293Ts

We conducted a CRISPR-Cas9-based genome-wide screen—involving a human CRIPSR activation pooled library (Synergistic Activation
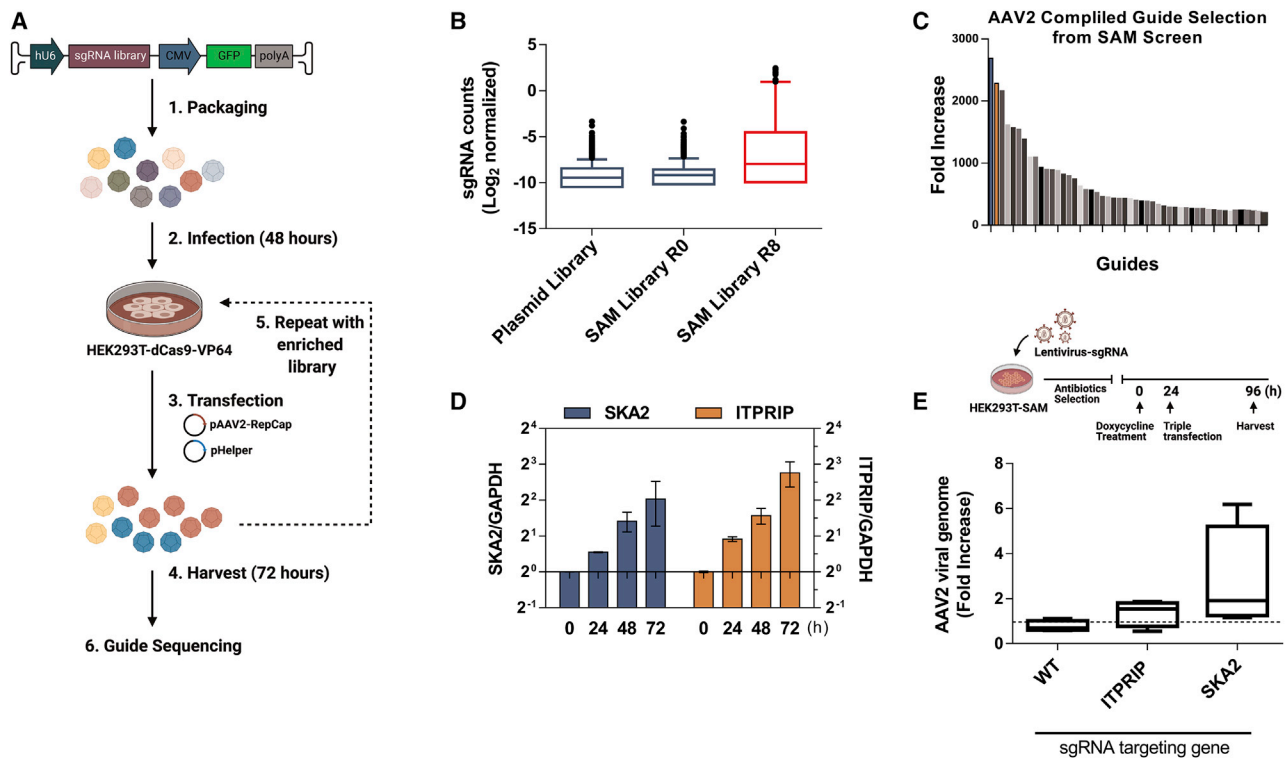
Figure 1. Parallel genome-wide screens identified candidate genes that increased HEK293 AAV manufacturing capacity

(A) Schematic of the iterative AAV-based selection with the Cas9-based SAM system to identify sgRNAs and corresponding candidate HEK293T gene targets, whose overexpression enhances AAV vector production. (B) Boxplots showing the distribution of SAM sgRNA frequencies before and after selection, showing that sgRNAs were enriched over eight rounds. Multiple sgRNAs were enriched after the selection rounds. Line: median; boxes, 25th to 75th percentiles; whiskers: 2.5th to 97.5th percentiles. (C) Compiled fold increase of the top 50 hits from each screen and their fold increase relative to the frequency in the pre-selected library. (D) mRNA induction levels of SKA2 and ITPRIP after triple plasmid transfection at indicated time points. Error bars, mean ± SD (E) Stable expression of SKA2 and ITPRIP sgRNA hits led to increases in AAV2 titer relative to WT HEK293Ts with no guide. HEK293T cells stably expression the SAM system were generated by lentivirus with doxycycline-inducible promoter and each sgRNA. Cell lines were treated with doxycycline for 24 h, followed by triple transfection for another 72 h. Line: median; boxes, 25th to 75th percentiles; whiskers: min/max.
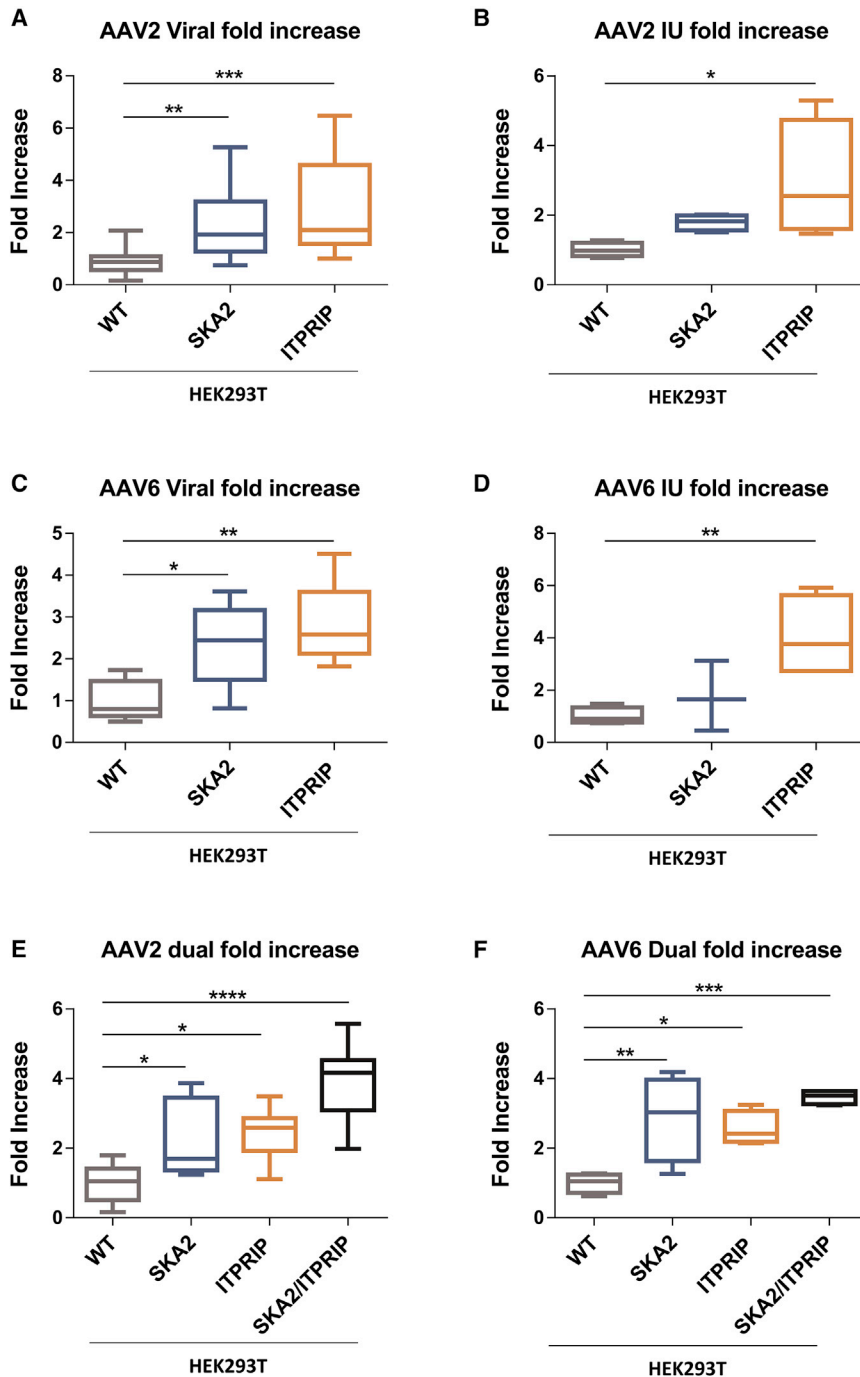
Mediator or SAM)[24]—to identify factors whose overexpression enhances AAV vector production. Specifically, a single-guide (sgRNA) library containing a total of 70,290 guide RNAs, to direct the SAM system to 23,430 human genes, was inserted into a recombinant AAV (rAAV) vector plasmid also encoding the green fluorescent protein (GFP). The SAM sgRNA AAV genome library was then packaged into recombinant AAV2 vector library, which was in turn used to infect HEK293T cells that stably expressed machinery necessary for gene activation with the SAM system (a dCas9-VP64 fusion with MS2-p65-HSF1). Infections were performed at a low multiplicity of infection (MOI) to limit the number of sgRNAs expressed per cell. After a 48-h incubation period to enable activation of the target genes, the cells were co-transfected with AAV-rep-cap and adenovirus helper plasmids to yield rAAV pools containing the library of sgRNAs from the SAM system, and this process constituted one round of selection. We hypothesized that rAAV clones encoding sgRNAs that directed SAM system toward cellular genes whose modulation enhanced rAAV production would be progressively enriched during successive rounds of selection. Therefore, the virus produced from each round of selection with the SAM library was used to re-infect the dCas9-VP64 expressing cells (Figure 1A), and again rescued

with helper plasmid transfection, for a total of 8 such selection rounds. Following this iterative selection with the SAM system, next-generation sequencing was used to determine the identities and relative frequencies of enriched sgRNAs (Figures 1B and 1C), which indicated a set of genetic targets whose gain-of-function appeared to increase AAV titers.

Stable cell line generation for verification of gRNA hits

The top hits from the sgRNA library targeted genes encoding the spindle and kinetochore associated complex subunit 2 (SKA2) transcript variant 2 and inositol 1, 4, 5-trisphosphate receptor interacting protein (ITPRIP) (Table S2). To characterize these targets further, we first analyzed whether expression of endogenous SKA2 and ITPRIP is modulated during AAV production, which could offer insights into whether these factors normally play a role in AAV packaging. Triple-plasmid-based AAV production increased transcription of SKA2 and ITPRIP (Figure 1D), suggesting that ectopic overexpression can offer further capacity for higher production.

We next generated stable HEK293T cell lines that express the sgRNA and SAM machinery. While HEK293T cells were used for the initial

A AAV2 Viral fold increase

B AAV2 IU fold increase

C AAV6 Viral fold increase

D AAV6 IU fold increase

E AAV2 dual fold increase

F AAV6 Dual fold increase

Figure 2. Cells expressing SKA2, ITPRIP, or both SKA2 and ITPRIP increased viral and infectious titer relative to HEK293 cells

Cells were seeded, and gene expression was induced 24 h before triple transfection with AAV packaging plasmids. Virus was harvested and titered by qPCR. (A) The fold increase in viral titer of AAV2 was determined in cell lines that expressed either SKA2 or ITPRIP in HEK293Ts (n = 21). (B) Increases in AAV2 infectious titer were also found in cells expressing either SKA2 or ITPRIP in HEK293Ts (n = 4). (C) Increases in AAV6 titer were found in both cells expressing either SKA2 or ITPRIP in HEK293Ts (n = 4). (D) Increase in AAV6 infectious titer was also found in both cells expressing either SKA2 or ITPRIP in HEK293Ts (n ≥ 3). (E) Fold increase of AAV2 packaged in a cell line that expresses both genes from the activation screen were able to increase titer by 3.8-fold compared to WT (n = 4). (F) Fold increase of AAV6 packaged in a cell line expressing both genes increased titer by 3.5-fold (n ≥ 4); all data shown $^*p \leq 0.05$, $^{**}p < 0.01$, $^{***}p \leq 0.005$, $^{****}p \leq 0.0005$ compared to WT. Line: median; boxes, 25th to 75th percentiles; whiskers: min/max.
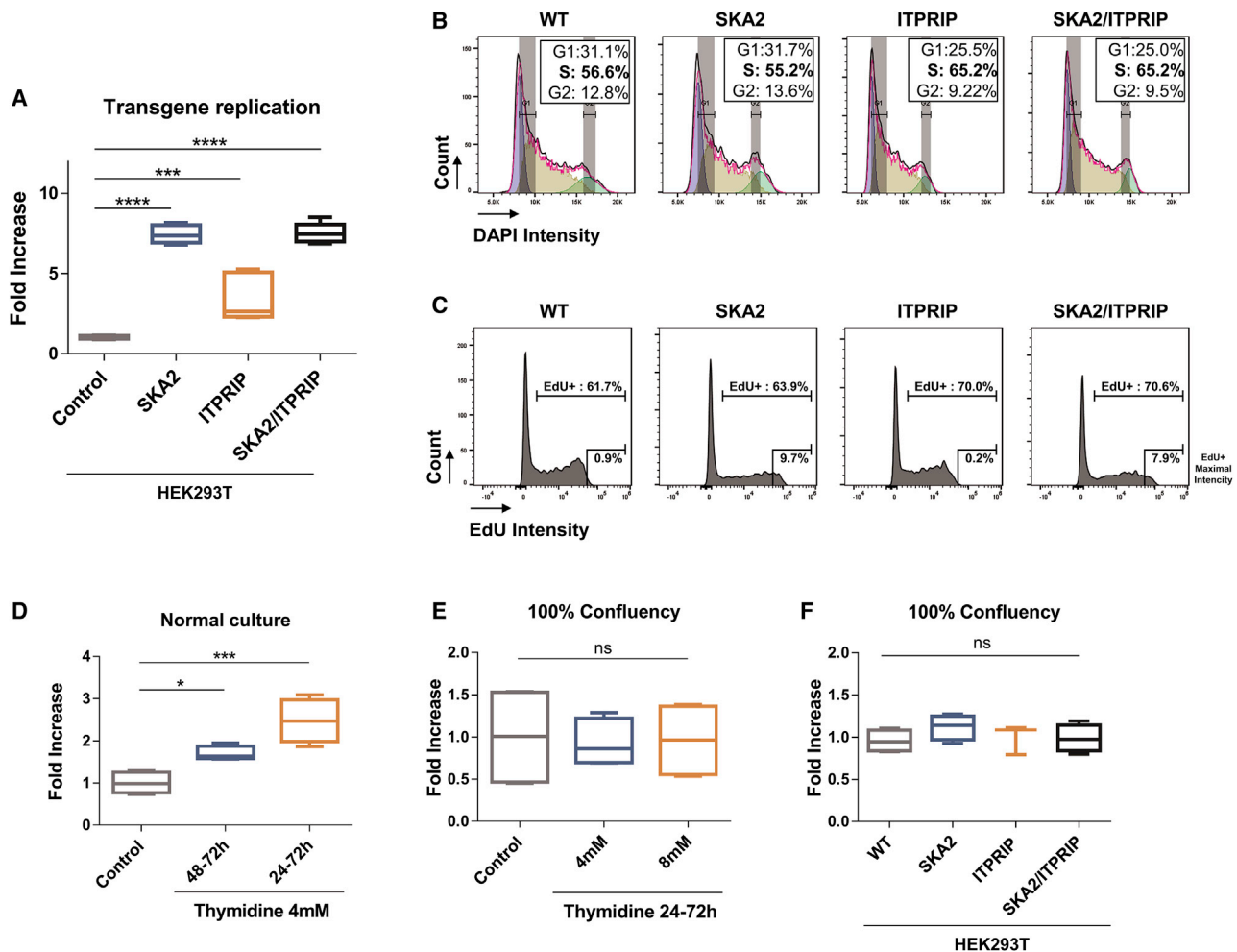
infectious titers of rAAV2 were significantly increased by 1.88- and 2.20-fold, respectively, when normalized to titers of HEK293T cells packaged in the same experiment (p ≤ 0.005) (Figures 2A and 2B). To determine whether this increase in titer could be generalized to other AAV serotypes, we used the same cell lines to produce AAV6, which packages among the lowest levels of natural AAV serotypes.[25] We observed similar fold increases in viral and infectious titers (Figures 2C and 2D). We next generated a dual SKA2 and ITPRIP over-expressing cell line and found it yielded a roughly additive increase of 3.8-fold in rAAV2 production and 3.5-fold in rAAV6 production (p ≤ 0.005; Figures 2E and 2F). Furthermore, this cell enabled increased production of AAV5 (1.9-fold) and AAV9 (4.6-fold; Figures S2B and S2C). Finally, we found that production following infection of WT AAV2 in the cell lines was elevated (Figures S3A and S3B), though not to as a high an extent as with recombinant vector production, indicating that SKA2 and ITPRIP modulates cellular function in a matter that promotes both vector production and WT AAV replication.

Effects of SKA2 and ITPRIP on biological processes that affect AAV production

SKA2 is a component of the SKA complex involved in cell-cycle progression and implicated in tumorigenesis, and its expression

selection and validation, further validation was conducted using HEK293s for generality. rAAV2 production was enhanced by up to 1.8-fold in these stable cell lines under standard rAAV packaging conditions, i.e., triple transfection including a GFP encoding vector plasmid in a 15 cm plate (Figure 1E). For further analysis and validation, HEK293 cell lines stably expressing the cDNA of the SKA2 and ITPRIP genes were generated (Figures S1A and S1B), and viral and
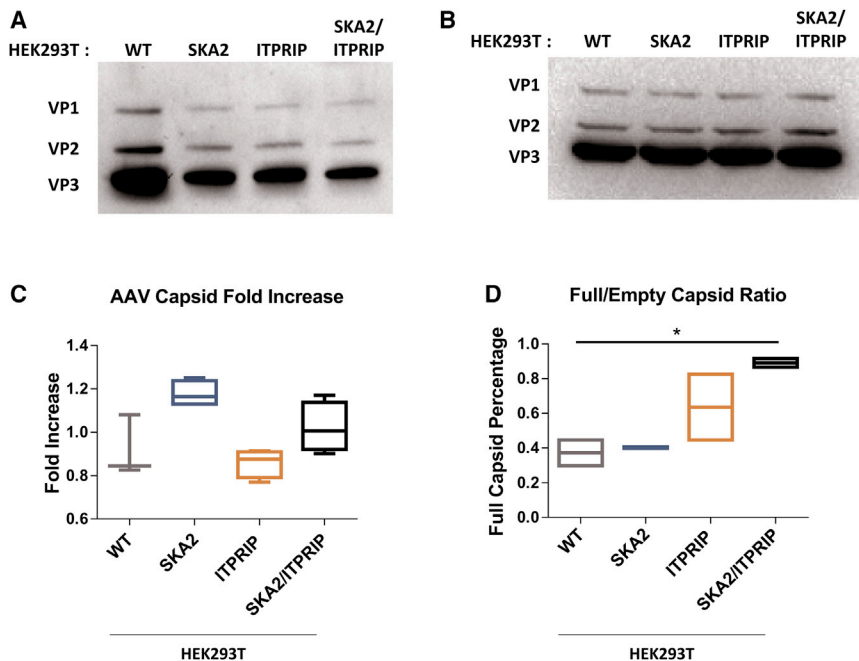
Figure 3. Overexpression of SKA2 and ITPRIP regulate AAV genome replication and cell cycle

(A) Fold increase of transgene replication at 2 days after triple transfection in the stable HEK293T cell lines (n ≥ 5). (B and C) Cell-cycle analysis by flow cytometry with DAPI staining (B) or EdU incorporation intensity (C) in the stable cell lines at day 2. (D) Fold increase of AAV2 packaged with thymidine treatment for 24 or 48 h. HEK293T cells were transfected for AAV packaging and treated with thymidine at the concentration of 4 mM (n = 4). (E) Comparison of AAV2 packaging with thymidine treatment from the HEK293T cells cultured at 100% confluency. Cells were transfected with AAV2 packaging genes, followed by thymidine treatment at 4 and 8 mM (n = 4). (F) AAV2 packaging changes in the stable cell lines cultured at 100% confluency (n = 4). For all data shown: *p ≤ 0.05, **p < 0.01, ***p ≤ 0.005, ****p ≤ 0.0005 compared to WT. Line: median; boxes, 25th to 75th percentiles; whiskers: min/max.

is regulated by p53 and by related cellular processes including DNA damage repair, cell-cycle checkpoints, and apoptosis.[26] ITPRIP enhances the calcium inhibitory function of IP3R, regulating intracellular calcium signaling.[27] To investigate how SKA2 and ITPRIP may enhance AAV packaging, we assessed numerous potential biological processes that could influence AAV production, including cell viability (Figures S4A and S4B), transfection efficiency (Figure S5A), and transcription of in-*trans*-supplied rAAV2 *cap* genes (Figure S5B) by trypan blue staining, flow cytometry, and quantitative PCR (qPCR), respectively. These processes were unaffected by expression of SKA2 and/or ITPRIP, suggesting that a potential later stage of AAV packaging could instead be affected.

Next, we examined the influence of SKA2 and ITPRIP on AAV vector genome replication by measuring the relative copy numbers of intracellular AAV transgene (ss-CAG-GFP) during vector production, as assessed via qPCR of episomal DNA isolated from cell lysate via Hirt extraction. AAV vector genome copies were significantly increased by ∼7.4, ∼3.4, and ∼7.5 fold in cells expressing SKA2, ITPRIP, and SKA2 plus ITPRIP, respectively (Figure 3A), indicating that these factors facilitate AAV genome replication.

Similar to other parvoviruses,[28,29] AAVs modulate the host cell cycle to facilitate viral genome replication.[30] For example, Rep78 arrests the cells in S-phase via multiple pathways,[31,32] and AAV2 genome replication occurs primarily in S/G2 phase.[33] We hypothesized SKA2 and/or

Figure 4. Overexpression of SKA2 and ITPRIP increase AAV full/empty capsid ratio

(A) HEK293T cell lysate was analyzed using western blot showing 1:1:10 ratio of VP1, VP2, and VP3 in different cell lines expressing SKA2, ITPRIP, or both SKA2 and ITPRIP, as well as WT HEK293Ts loaded with equivalent vgs (1×10^9). (B) Western blot under the same conditions but instead loading equal protein concentrations (20 μg). (C) AAV2 capsid fold increase relative to WT HEK293Ts in each of the cell lines as quantified by ELISA (n ≥ 3). One-way ANOVA analysis indicated no statistical differences. (D) Ratio of AAV2 viral genomes to capsids in WT cell lines or cell lines expressing SKA2, ITPRIP, or both. One-way ANOVA analysis showed a significant difference between groups expressing SKA2 and ITPRIP compared to the WT (n ≥ 3, p ≤ 0.05). Line: median; boxes, 25th to 75th percentiles; whiskers: min/max.

ITPRIP may modulate the cell cycle in a manner that increases AAV genome replication, resulting in increased AAV titer. Flow cytometric analysis of 4′,6-diamidino-2-phenylindole (DAPI) staining revealed that cell-cycle distribution was similar for normally propagating WT, SKA2-, and ITPRIP-expressing cell lines (Figure S6). However, we next assessed the cell-cycle population during viral production. 2 days after transfection, flow cytometric analysis of DAPI staining and EdU incorporation showed that the S-phase population was increased in ITPRIP-expressing cell lines (Figures 3B and 3C). Moreover, a fraction of cells shifted toward higher EdU incorporation in the SKA2-expressing cell lines, suggesting that SKA2 increases DNA replication or exerts other cell-cycle effects.[34] Given the effects of Rep78 and ITPRIP on the proportion of cells in S phase, we used the cell-cycle inhibitor thymidine to arrest cells in S-phase after triple transfection (Figure S6). Thymidine-mediated S-phase arrest increased AAV production by ∼1.6 and ∼2.4 fold depending on treatment period (Figure 3D). To assess whether thymidine's effect was mediated through the cell cycle, we cultured cells at 100% confluency to arrest them in G0/G1-phase, followed by triple transfection and thymidine treatment. Thymidine did not increase the AAV titer under these conditions (Figure 3E), suggesting that it affects the AAV titer by modulating cell cycle. Finally, we tested the AAV production efficiency of the stable cell lines arrested in G0/G1-phase. Unlike normally cultured cells (Figures 2A–2F), SKA2 and ITPRIP expression did not increase AAV titer in cells at 100% confluency (Figure 3F). Taken together, our data indicate SKA2 and ITPRIP increase AAV titer by affecting host cell cycle to facilitate AAV vector genome replication.

AAV packaging efficiency in producer cell lines

Following viral genome replication, the lower molecular weight Rep proteins promote genome encapsidation into AAV virion to generate

infectious AAV.[35] We examined whether increased AAV vector genome replication may in turn increase the efficiency of viral genome loading into AAV in SKA2 and ITPRIP expressing cell lines. The AAV in crude lysate was analyzed via western blot, ELISA, and qPCR to compare relative capsid and viral genome levels. 1×10^9 AAV2 viral genomes were analyzed via western blot for VP1, 2, and 3, and the WT had higher capsid band intensity than vector generated in the three engineered cell lines, indicating a higher amount of protein per genome, potentially due to a higher empty/full ratio. Loading equal protein levels, rather than an equal genome levels, led to very similar band intensities (Figures 4A and 4B). To complement the western, ELISA quantification of capsid levels produced in each of the lines was statistically the same (Figure 4C). Finally, comparing the genomic titers to the capsid levels revealed that while the WT and SKA2 overexpressing lines had similar full/empty vector ratios (0.37 and 0.40, respectively), the two lines overexpressing ITPRIP showed significant increases in the proportion of full virions by up to 2.4-fold (0.63 and 0.89, respectively; Figure 4D). These results collectively indicate that increased vector genome replication promotes genome packaging into virions, resulting in a higher proportion of full AAV virions.

DISCUSSION

A genome-wide transcriptional activation library coupled with selective pressure for increased AAV production identified targets that increase AAV manufacturing capacity. Upregulation of several such key targets not only with a Cas9-based transactivation system but also cDNA overexpression of the corresponding target increased AAV production nearly 3-fold. Furthermore, a cell line that combined two key hits increased production up to 4-fold, a clinically meaningful result. Finally, during AAV production in these cell lines, both vector genome replication and the subsequent full virion percentage were elevated, potentially due to modulation of the cell cycle.

The most enriched sgRNA's in the SAM library targeted SKA2 and ITPRIP. Current knowledge of these genes does not suggest a

common biological pathway, and the finding that SKA2 and ITPRIP additively increase AAV production suggests independent mechanisms. SKA2 is part of a complex necessary for proper chromosome segregation during the transition between metaphase and anaphase and plays a role in spindle checkpoint silencing.[26,36] AAV Rep proteins have been shown to arrest cells in the S-phase, during which AAV replication occurs.[31–33] Because DNA replication during S-phase delays the timing of mitosis[37] and the spindle assembly checkpoint is activated during S-phase,[37] SKA2 may influence cell-cycle kinetics by affecting the spindle assembly checkpoint to increase the replication of AAV vector genome, resulting in higher AAV titer and percentage of full AAV virions. SKA2 has three transcript variants, with alternative C-termini, due to the alternative splicing and a different ORF.[26] In this study, we expressed SKA2 transcript variant two in accordance with annotation of the SAM library sgRNA,[24] which targets the transcription starting site of SKA2 transcription variant two (GenBank: NM_001100595.1). However, an updated NCBI Reference Sequence (GenBank: NM_001100595.2) indicates that the exon 1 starting sequence of SKA2 transcription variant two is same as the other SKA2 transcription variants, suggesting that the enriched sgRNA could upregulate all variants. Our ongoing studies may determine possible effects of other SKA2 transcription variants on AAV packaging.

ITPRIP binds to the ITP receptor in the endoplasmic reticulum (ER) membrane and enhances its sensitivity to intracellular calcium signaling.[27] It has been shown to influence intracellular calcium release by interacting with the ITP receptor, localizing to the nuclear envelope, and thereby potentially controlling the nuclear calcium level.[38] Calcium signaling modulates cell-cycle progression[39] and DNA damage responses,[40] which suggests a potential mechanism wherein ITPRIP can promote AAV production by regulating intracellular or intranuclear calcium.

AAV replication is linked to the cell cycle and the activation of signaling molecules that mediate cell-cycle arrest, i.e., checkpoint kinase 1 (CHK1), CHK2, and structural maintenance of chromosomes protein 1 (SMC1).[41] Our study showed that upregulation of SKA2 and ITPRIP increases viral genome replication (Figure 3A), influences the cell cycle (Figures 3B and 3C), and increases the ratio of the full/empty AAV virion (Figure 4D). Moreover, thymidine, which arrests cells in S-phase and activates CHK1, CHK2, and SMC1,[42] increased AAV titer (Figure 3D). These effects were abrogated when cells were arrested in G0-phase (Figure 3E), suggesting that these proteins increase AAV transgene replication by regulating the cell cycle or activating cell-cycle-related molecules. Taken together, the unbiased screening approach applied in this study highlights potential mechanisms for enhancement of AAV production that are not inherently linked to previously described AAV packaging pathways.

Our study also showed that combinatorial targeting of multiple hits is feasible and effective. That is, a stable cell line expressing both SKA2 and ITPRIP produced more AAV than lines expressing either individual protein (Figures 2E and 2F). The SKA2/ITPRIP-expressing cell line had features of both SKA2 and ITPRIP expressing cell lines. That is, elevated S-phase synthesis was observed in the SKA2-expressing cell line (Figure 3C), and flow analysis showed that the S-phase population was increased in the ITPRIP expressing-cell line during AAV production (Figures 3B and 3C). Combining additional targets that operate via alternative pathways or mechanisms may therefore further boost production.

In addition to overall productivity, a key issue that AAV manufacturing processes face is the presence of empty capsids, which increase viral protein antigen load and thereby raise immune response concerns,[43] as well as potentially competitively inhibit transduction by genome-containing virions. While gradient ultracentrifugation can eliminate empty capsids, it is not readily scalable. In addition, ion exchange chromatography can reduce, but not completely eliminate, empty capsids.[44] Overexpressing ITPRIP cDNA either singly or especially in combination with SKA2 increased the fraction of full capsids from 0.4 to 0.6 or 0.9, respectively. Based on ELISA data, the number of capsids remained relatively constant while the viral genome levels increased. Future work may explore the underlying mechanisms.

In addition to affecting manufacturing yield, a producer cell can modulate properties of the resulting AAV virions. For example, Sf9 cells can apparently alter capsid molecular weights, process-specific residuals, and infectivity.[45] Likewise, overexpression or downregulation of specific host proteins in producer cell line can modulate transcription and post-translational modifications of AAV proteins,[46–48] which can in turn conceivably alter virion assembly or infectivity. However, the engineered cell lines were report here are capable of generating higher titers of vector at similar to genome/infectious ratios as unmodified cells (Figures 2B, 2D, and 2F).

There are several potential additional directions for future study. While selections were originally conducted using AAV2, the screen showed that improved production extended to AAV6, AAV5, and AAV9, suggesting that a common biological mechanism applies to multiple serotypes. Additional serotypes and variants can be tested in the future. In addition, hits arising from a screen in standard adherent mammalian culture may not extend to high surface area or suspension bioreactors. However, hits arising in a HEK293T screen also functioned in HEK293s, suggesting some level of generality of the hits, and the screen is relatively rapid and could be repeated for different culture systems, cell lines (e.g., HeLa, Sf9), or even viral vectors.

This genome-wide screen demonstrates that cells can be optimized for viral manufacturing by selecting for guides that modulate expression of target genes to enhance viral production, which improves the economics of vector manufacturing and takes steps toward extending the benefits of AAV gene therapy to larger patient populations. Furthermore, our approach can identify host genes that regulate virion production, leading to advances in basic knowledge of viral replication and potentially the future capacity to rationally design producer cell lines.

MATERIALS AND METHODS

Study design

The objective of this study was to determine whether cellular gene expression could be altered to increase the AAV production capabilities of that line, as well as to verify that those changes were not an artifact of the selection process. We used an AAV packaged library of CRISPR guide RNAs together with cell lines expressing activation (dCas9-VP64/MS2-p65-HSF1) machinery to conduct tandem screens for genetic perturbations that increased AAV manufacturing capacity. Cells were infected and allowed 48 h for guide onset, after which the cells were transfected with AAV packaging plasmid to repackage the sgRNA-containing AAV genomes and thereby generate an AAV vector library enriched with advantageous sgRNAs, after which the selection could be repeated. After eight rounds of selection, next generation sequencing was used to compare the prevalence of guides in the original packaged library with the prevalence of guides in the final library. The top hits from this analysis were then used to create cell lines that stably expressed both the guide RNA and the CRISPR machinery to validate AAV packaging increase. Further validation was done by expressing cDNA of the two top guides from the activation screen and evaluating AAV packaging increases.

rAAV CRISPR-Cas9 cell line development

To modulate cellular activity, we used a HEK293T cell line that constitutively expresses both a deactivated Cas9 fused to VP64 and the activation helper proteins MS2-p65-HSF1 by infection with lentivirus vectors packaged with lenti dCAS-VP64_Blast (Addgene Plasmid #61425) and lenti MS2-p65-HSF1_Hygro (Addgene Plasmid #61426) and selection using both hygromycin and blastomycin.

In addition, the hU6 promoter and sgRNAs from the SAM plasmid library of lenti sgRNA(MS2)_zeo (Addgene Plasmid #61427) were cloned into a self-complementary rAAV backbone to generate the hU6-SAMsgRNA-CMV-GFP rAAV library. Electroporation of the library ligation reaction into *E. coli* resulted in a library diversity (5×10^6 colonies), which ensured the full library was represented. These SAM rAAV library expresses both the single-guide RNAs for gene targeting (from the hU6 promoter) and a GFP reporter (from CMV) used to monitor rAAV infection.

AAV library preparation

HEK293T cells were obtained from the American Type Culture Collection (Manassas, VA, USA) and cultured in DMEM (GIBCO) with 10% fetal bovine serum (Invitrogen) and 1% penicillin/streptomycin/Amphtericin B (GIBCO) at 37°C and 5% CO_2. AAV vector libraries were packaged containing the sgRNA library driven by the hU6 promoter, as well as GFP driven by the cytomegalovirus (CMV) promoter. These vectors were packaged in HEK293T cells as previously described.[49,50]

To package AAV from these lines, we seeded HEK293Ts at a density of 10 million cells per 15 cm dish and grown until they reached approximately 80% confluency. Cells were then triple transfected using the standard triple transfection technique with rAAV2 packaging ss-CAG-GFP.[51] 72 h later, cells were harvested, and the supernatant was collected. The cell pellet was resuspended in 50 mM Tris and 150 mM NaCl with pH 8.5 before being freeze/thawed three times (−80°C/ 37°C). 1 U/μL Benzonase was added, and lysate was incubated at 37°C for 30 min. The lysate was spun at $500 \times g$ for 2 min, and the supernatant was collected and spun again at $10,000 \times g$ for 10 min. Virus in the supernatant was precipitated with 8% v/v PEG and 0.5 mM NaCl. After 24 h at 4°C, the supernatant was spun at $4,000 \times g$ for 20 min and combined with cell lysate. From there, the virus was quantified.

qPCR

qPCR was used to quantify the genome-containing particle titer via SYBR Green, 3 mM $MgCl_2$, 0.2 mM dNTP, and Jump Start Taq on a CFX RT PCR machine (Bio-Rad). Plasmid DNA was used from a concentration of 1 ng/μL to 0.0001 ng/μL to generate a standard curve with primers against GFP (5′-ACTACAACAGCCACAACGTCTA TATCA-3′ and 5′-GGCGGATCTTGAAGTTCACC-3′). Each condition was run with two technical duplicates and where each biological replicate was a separately transfected 15 cm dish, where the number of plates ranged from n = 4 to n = 22. To measure the mRNA induction of SKA2, ITPRIP, and *cap* in response to triple transfection, we isolated total mRNA using RNeasy mini kit (QIAGEN), followed by cDNA synthesis using iScript cDNA Synthesis kit (Bio-Rad) in accordance with manufacturer's protocol. qPCR was performed using gene specific primer pairs for SKA2 (5′-CCGCTTTAAACCAGTTGC TG-3′, 5′-CTCTGCCGCAGTTTTCTCTT-3′), ITPRIP (5′-AGTCTG GCCCAGTTCAGAGA-3′, 5′-CGCTGGAGTGAGGAACTAGG-3′), *cap* (5′-CACCTTCAGTGCGGC-3′, 5′-GTACTCCACGGGACA GGTCAG-3′), and glyceraldehyde-3-phosphate dehydrogenase (GAPDH, 5′-TGACCACAGTCCATGCCAT-3′, 5′- GACGGACAC ATTGGGGGTAG-3′). mRNA expression was normalized to GAPDH and calculated using delta-delta threshold cycle method.

In vitro selections for single-guide RNA sequences that either activate or knockout genes to increase AAV packaging

To select for guides that increased a cellular AAV packaging capacity, the guide libraries were first packaged into rAAV2 through the standard triple transfection technique (pXX2-AAV2, pHelper, hU6-SAM sgRNA-CMV-GFP library) in WT HEK293Ts and titered via qPCR. The resulting knockout or activation AAV libraries were then used to infect the cell lines expressing dCas9-VP64 MS2-p65-HSF1. The knockout and activation selections were then conducted separately, but the process was the same. During the first round of selection, the 293T cell lines were infected at a range of MOIs (25–2,000) in 24-well plate format (500,000 cells). Because rAAV has an infectious particle-to-viral genome ratio of 1:100–1:1,000, we targeted a viral genomic MOI of 50–500 to achieve approximately 30% GFP-positive cells. A MOI of 500 was selected for subsequent rounds of selection because it most closely satisfied the 30% GFP-positive criteria. The infected cell lines were incubated for 48 h to allow for onset of sgRNA expression and Cas9-mediated targeting of a given

specific guide to its corresponding gene. GFP reporter expression from the same AAV vector was used to ensure onset of gene expression and measure transduction efficiency. The intracellular AAV vector genomes were then repackaged by a double transfection of pXX2-AAV2 and pHelper. rAAVs that encoded sgRNAs directed toward production enhancing genes would be progressively enriched during rounds of selection. After each round, virus was used to re-infect the dCas9-VP64 or Cas9 expressing cells and the selection process was repeated.

As an intermediate step to recover and clone the sgRNA libraries, genomic DNA was extracted from the cells after round 5, respectively, PCR was used to amplify the sgRNA library, and the resulting fragments were re-cloned into the rAAV backbone. This library was then packaged as in round 1 to generate vector for infection in round 6, respectively. Three additional rounds of selection were conducted, after which samples from the plasmid library, packaged AAV library (prior to selection), and rounds 5 and 8 of the SAM selection were deep sequenced to identify the sgRNA sequences that were most enriched after selection.

Next-generation sequencing of sgRNA libraries
Next-generation sequencing of the SAM library was performed to evaluate the fold enrichment of each sgRNA sequence after completion of AAV packaging selections. Primers used for library preparation are listed in Table S1. Nine NGS-hU6-Fwd primers were designed, each containing 1–9 additional nucleotides to function as a barcode. Each sgRNA library was amplified by PCR using Phusion High-Fidelity DNA polymerase (NEB), and PCR products were gel purified using the PureLink Quick Gel Extraction and PCR purification Combo Kit (Thermo-Fisher) according to manufacturer instructions. The barcoded amplicons were then pooled and sequenced at the QB3 Vincent J. Coates Genomics Sequencing Laboratory at UC Berkeley using the MiSeq platform and TruSeq SBS Kit v3-HS (Illumina). Illumina FASTQ files were demultiplexed, and adaptor sequences were trimmed. The resulting demultiplexed sequences were analyzed using Python scripts to identify each sgRNA and determine its frequency. Identification of each sgRNA was performed using custom script, and using the reference files SAM.tsv, sgRNA counts were then compiled using the Python script count_sgrna.py (Table S1).

Analysis and validation of gRNA hits
Cells expressing dCas9-VP64 and MS2-p65-HSF1 cells were infected with lenti sgRNA(MS2)_zeo (Addgene plasmid #61427) containing the guides activating ITPRIP or SKA2. Cells with a stable integration event were then selected with zeomycin.

In addition to validating the sgRNAs for transcriptional activation of endogenous ITPRIP or SKA2, WT 293Ts were infected with lentivirus pCW57.1 (Addgene plasmid #41393) for doxycycline-inducible expression of the cDNAs that correspond to the upregulated guides in the SAM selection. Doxycycline was added to the cells 2 days before packaging to induce cDNA expression.

AAV infectious titering
10,000 HEK293T cells were seeded in a 96-well plate. 24 h later, a serial dilution of virus encoding ss-CAG-GFP was used to infect these cells, and after 24 h GFP$^+$ cells and total cells were quantified using an ImageXpress Micro imaging system (IXM). All cells were infected with dilutions of virus such that the fraction of cells that were GFP positive were below 20%. Infectious titer was calculated as the % GFP$^+$ cells multiplied by the total cell number and divided by the volume of viral solution added to a well, and this titer was calculated from the average of two vector dilutions.

Cell-cycle analysis
Cell cycle was evaluated by DAPI staining and EdU incorporation assay. For DAPI staining, cells were harvested using Accutase (Stem Cell) and incubated on ice with 70% ice-cold ethanol. 30 min later, samples were washed with PBS containing 2 mM EDTA and 5% FBS and incubated with DAPI solution at 1 μg/mL (Sigma) for 10 min.

EdU incorporation assay was performed with Click-iT EdU Flow Cytometry Assay Kit from Invitrogen in accordance with the protocol. Briefly, cells were incubated with 10 μM of EdU for 1 h and harvested. Samples were washed and sequentially incubated with reagent for fixation, permeabilization, and stained by the reaction cocktail containing Alexa Fluor 488 azide. After incubation in dark for 30 min, samples were washed and analyzed by flow cytometry using Attune NxT flow cytometer. Data were analyzed using FlowJo v.10.7.1

AAV gene replication
Isolation of episomal DNA for the analysis of AAV transgene replication was performed as previously described.[52] HEK293T cells were seeded in 10 cm dish and transfected with AAV packaging genes including ss-CAG-GFP. 48 h after triple transfection, cells were harvested and washed with DPBS. The cell pellet was incubated with 500 μL of Hirt lysis buffer for 10 min RT and followed by proteinase K digestion (50 μg/mL final concentration) for 1 h at 37°C. The reaction was stopped by adding 120 μL of 5 M NaCl, and tubes were kept at 4°C overnight to precipitate chromosomal DNA. Next day, samples were centrifuged for 1 h (17,000 g, 4°C), the supernatant was transferred to new tubes, and phenol/chloroform/isoamyl alcohol mixture (Sigma) was added. After centrifuging for 10 min, the upper layer was transferred, and sodium acetate was added. After overnight incubation at −20°C, the dried pellets were re-suspended with nuclease-free DW after washing with 70% ethanol. 1 μg of DNA was digested with DpnI (NEB) for 2 h at 37°C, followed by heat inactivation at 80°C for 20 min. qPCR was performed to measure the amount of replicated transgene using primers for ss-CAG-GFP.

Cell-cycle arrest
Thymidine (Sigma) was dissolved in DMSO at 200 mM and added to cells 24 h after triple transfection (final concentration: 4 and 8 mM). For G1-phase arrest, 600,000 cells were seeded on 10 cm dish and incubated for 48 h to reach 100% confluency and incubated another 24 h. Cells were transfected for AAV packaging and titer was measured as described in the qPCR section.

Cell viability

Cells were harvested after triple transfection and diluted in PBS then stained with 0.4% trypan blue (Invitrogen) at a 1:1 ratio. Samples were mounted onto the hemocytometer to count the viable cells. Cell viability by the TO-PRO-3 (Thermo Fisher) stain was performed with the manufacturer's protocol and analyzed using flow cytometry (Excitation/Emission: 642/661 nm).

AAV vector characterization

AAV2 ELISAs were done according to the manufacturer's protocol (PROGEN, AAV Titration ELISA 2.0R) against assembled capsids. Each sample was diluted $1,000\times$ and $100\times$ and run in technical duplicates with four biological replicates for each condition. Capsids were also analyzed via western blot, loading either 1×10^9 capsids or 20 µg of crude lysate. Mouse anti-VP1-3 monoclonal antibody, B1 (PROGEN) was used at a dilution of 1:300 and analyzed via horseradish peroxidase-conjugated secondary antibodies (1:5,000), followed by enhanced chemiluminescence (ECL) detection.

Statistical analysis

All comparisons were performed using Prism 8 (GraphPad Software). AAV viral and infectious titers were compared using a one-way ANOVA and comparisons between different groups were doing using a Dunnett's multiple comparisons test.

SUPPLEMENTAL INFORMATION

Supplemental information can be found online at https://doi.org/10.1016/j.omtn.2021.06.026.

AUTHOR CONTRIBUTIONS

D.V.S. supervised the entire project. C.R.B. and H.L. performed most of the experiments, analyzed the data, and wrote the manuscript with help from D.V.S. D.S.O. and D.V.S. conceived the screening strategy. C.R.B. and D.S.O. performed the screening and analyzed the sequencing data. K.K.L. contributed to early revisions and conducting AAV production experiments. P.L. created the cell line in which all experiments were conducted and assisted in developing the system and conducting AAV production experiments.

DECLARATION OF INTERESTS

C.R.B., D.S.O., and D.V.S. are inventors on patents related to cell lines for increased production of AAV. D.V.S. is a co-founder of 4D Molecular Therapeutics.

REFERENCES

1. O. of the Commissioner (2019). FDA approves innovative gene therapy to treat pediatric patients with spinal muscular atrophy, a rare disease and leading genetic cause of infant mortality. FDA. https://www.fda.gov/news-events/press-announcements/fda-approves-innovative-gene-therapy-treat-pediatric-patients-spinal-muscular-atrophy-rare-disease.

2. O. of the Commissioner (2017). Press Announcements - FDA approves novel gene therapy to treat patients with a rare form of inherited vision loss. FDA. https://www.fda.gov/newsevents/newsroom/pressannouncements/ucm589467.htm.

3. Spark Therapeutics LUXTURNA package insert. 1–16.

4. AveXis (2019). ZOLGENSMA® (onasemnogene abeparvovec-xioi) suspension for intravenous infusion [package insert]. Bannockburn (IL): AveXis Inc; 2019 May. Available from: https://www.fda.gov/media/126109/download. 1–14.

5. Gene Transfer Clinical Trial to Deliver rAAVrh74.MCK.GALGT2 for Duchenne Muscular Dystrophy ClinicalTrials.gov. https://clinicaltrials.gov/ct2/show/NCT03333590.

6. Phase, A. 3 Study to Evaluate the Safety and Efficacy of PF-06939926 for the Treatment of Duchenne Muscular Dystrophy ClinicalTrials.gov. https://clinicaltrials.gov/ct2/show/NCT04281485.

7. Safety and Dose-Finding Study of DTX401 (AAV8G6PC) in Adults With Glycogen Storage Disease Type Ia (GSDIa) ClinicalTrials.gov. https://clinicaltrials.gov/ct2/show/record/NCT03517085.

8. HOPE-B Trial of AMT-061 in Severe or Moderately Severe Hemophilia B Patients ClinicalTrials.gov. https://clinicaltrials.gov/ct2/show/NCT03569891.

9. Single-Arm Study To Evaluate The Efficacy and Safety of Valoctocogene Roxaparvovec in Hemophilia A Patients ClinicalTrials gov. https://clinicaltrials.gov/ct2/show/record/NCT03370913.

10. Study of Intrathecal Administration of Onasemnogene Abeparvovec-xioi for Spinal Muscular Atrophy ClinicalTrials gov. https://clinicaltrials.gov/ct2/show/NCT03381729.

11. Systemic Gene Delivery Clinical Trial for Duchenne Muscular Dystrophy ClinicalTrials.gov.

12. Duan, D. (2018). Systemic AAV Micro-dystrophin Gene Therapy for Duchenne Muscular Dystrophy. Mol. Ther. 26, 2337–2356.

13. Nance, M.E., and Duan, D. (2015). Perspective on adeno-associated virus capsid modification for duchenne muscular dystrophy gene therapy. Hum. Gene Ther. 26, 786–800.

14. Menolfi, D., and Zha, S. (2020). ATM, ATR and DNA-PKcs kinases-the lessons from the mouse models: inhibition ≠ deletion. Cell Biosci. 10, 8.

15. Kaspar, B.K., Gardell, B., Chung, K., Vallabhaneni, D., and Legmann, R. (2019). Assessment of an Adherent HEK293 Cell Transfection Process for Scalable AAV Production in the iCELLis (R) 500 Fixed-Bed Bioreactors. Mol Ther 27, 226–227.

16. Dalkara, D., Byrne, L.C., Klimczak, R.R., Visel, M., Yin, L., Merigan, W.H., Flannery, J.G., and Schaffer, D.V. (2013). In vivo-directed evolution of a new adeno-associated virus for therapeutic outer retinal gene delivery from the vitreous. Sci. Transl. Med. 5, 189ra76.

17. Steines, B., Dickey, D.D., Bergen, J., Excoffon, K.J.D.A., Weinstein, J.R., Li, X., Yan, Z., Abou Alaiwa, M.H., Shah, V.S., Bouzek, D.C., et al. (2016). CFTR gene transfer with AAV improves early cystic fibrosis pig phenotypes. JCI Insight 1, e88728.

18. Zinn, E., Pacouret, S., Khaychuk, V., Turunen, H.T., Carvalho, L.S., Andres-Mateos, E., Shah, S., Shelke, R., Maurer, A.C., Plovie, E., et al. (2015). In silico reconstruction of the viral evolutionary lineage yields a potent gene therapy vector. Cell Rep. 12, 1056–1068.

19. Guenther, C.M., Brun, M.J., Bennett, A.D., Ho, M.L., Chen, W., Zhu, B., Lam, M., Yamagami, M., Kwon, S., Bhattacharya, N., et al. (2019). Protease-Activatable Adeno-Associated Virus Vector for Gene Delivery to Damaged Heart Tissue. Mol. Ther. 27, 611–622.

20. Clément, N., and Grieger, J.C. (2016). Manufacturing of recombinant adeno-associated viral vectors for clinical trials. Mol. Ther. Methods Clin. Dev. 3, 16002.

21. Naumer, M., Sonntag, F., Schmidt, K., Nieto, K., Panke, C., Davey, N.E., Popa-Wagner, R., and Kleinschmidt, J.A. (2012). Properties of the adeno-associated virus assembly-activating protein. J. Virol. 86, 13038–13048.

22. Wang, X.S., Ponnazhagan, S., and Srivastava, A. (1996). Rescue and replication of adeno-associated virus type 2 as well as vector DNA sequences from recombinant

plasmids containing deletions in the viral inverted terminal repeats: selective encapsidation of viral genomes in progeny virions. J. Virol. 70, 1668–1677.

23. Wang, X.S., Qing, K., Ponnazhagan, S., and Srivastava, A. (1997). Adeno-associated virus type 2 DNA replication in vivo: mutation analyses of the D sequence in viral inverted terminal repeats. J. Virol. 71, 3077–3082.

24. Konermann, S., Brigham, M.D., Trevino, A.E., Joung, J., Abudayyeh, O.O., Barcena, C., Hsu, P.D., Habib, N., Gootenberg, J.S., Nishimasu, H., et al. (2015). Genome-scale transcriptional activation by an engineered CRISPR-Cas9 complex. Nature 517, 583–588.

25. Mietzsch, M., Grasse, S., Zurawski, C., Weger, S., Bennett, A., Agbandje-McKenna, M., Muzyczka, N., Zolotukhin, S., and Heilbronn, R. (2014). OneBac: platform for scalable and high-titer production of adeno-associated virus serotype 1-12 vectors for gene therapy. Hum. Gene Ther. 25, 212–222.

26. Xie, M., and Bu, Y. (2018). SKA2/FAM33A: A novel gene implicated in cell cycle, tumorigenesis, and psychiatric disorders. Genes Dis. 6, 25–30.

27. van Rossum, D.B., Patterson, R.L., Cheung, K.H., Barrow, R.K., Syrovatkina, V., Gessell, G.S., Burkholder, S.G., Watkins, D.N., Foskett, J.K., and Snyder, S.H. (2006). DANGER, a novel regulatory protein of inositol 1,4,5-trisphosphate-receptor activity. J. Biol. Chem. 281, 37111–37116.

28. Chen, A.Y., and Qiu, J. (2010). Parvovirus infection-induced cell death and cell cycle arrest. Future Virol. 5, 731–743.

29. Ganaie, S.S., and Qiu, J. (2018). Recent advances in replication and infection of human parvovirus B19. Front. Cell. Infect. Microbiol. 8, 166.

30. Winocour, E., Callaham, M.F., and Huberman, E. (1988). Perturbation of the cell cycle by adeno-associated virus. Virology 167, 393–399.

31. Saudan, P., Vlach, J., and Beard, P. (2000). Inhibition of S-phase progression by adeno-associated virus Rep78 protein is mediated by hypophosphorylated pRb. EMBO J. 19, 4351–4361.

32. Berthet, C., Raj, K., Saudan, P., and Beard, P. (2005). How adeno-associated virus Rep78 protein arrests cells completely in S phase. Proc. Natl. Acad. Sci. USA 102, 13634–13639.

33. Franzoso, F.D., Seyffert, M., Vogel, R., Yakimovich, A., de Andrade Pereira, B., Meier, A.F., Sutter, S.O., Tobler, K., Vogt, B., Greber, U.F., et al. (2017). Cell Cycle-Dependent Expression of Adeno-Associated Virus 2 (AAV2) Rep in Coinfections with Herpes Simplex Virus 1 (HSV-1) Gives Rise to a Mosaic of Cells Replicating either AAV2 or HSV-1. J. Virol. 91, 1–19.

34. Pereira, P.D., Serra-Caetano, A., Cabrita, M., Bekman, E., Braga, J., Rino, J., Santus, R., Filipe, P.L., Sousa, A.E., and Ferreira, J.A. (2017). Quantification of cell cycle kinetics by EdU (5-ethynyl-2′-deoxyuridine)-coupled-fluorescence-intensity analysis. Oncotarget 8, 40514–40532.

35. Bennett, A., Mietzsch, M., and Agbandje-Mckenna, M. (2017). Understanding capsid assembly and genome packaging for adeno-associated viruses. Future Virol. 12, 283–297.

36. Hanisch, A., Silljé, H.H.W., and Nigg, E.A. (2006). Timely anaphase onset requires a novel spindle and kinetochore complex comprising Ska1 and Ska2. EMBO J. 25, 5504–5515.

37. Magiera, M.M., Gueydon, E., and Schwob, E. (2014). DNA replication and spindle checkpoints cooperate during S phase to delay mitosis and preserve genome integrity. J. Cell Biol. 204, 165–175.

38. Cheng, L.C., Baboo, S., Lindsay, C., Brusman, L., Martinez-Bartolomé, S., Tapia, O., Zhang, X., Yates, J.R., 3rd, and Gerace, L. (2019). Identification of new transmembrane proteins concentrated at the nuclear envelope using organellar proteomics of mesenchymal cells. Nucleus 10, 126–143.

39. Kahl, C.R., and Means, A.R. (2003). Regulation of cell cycle progression by calcium/calmodulin-dependent pathways. Endocr. Rev. 24, 719–736.

40. Görlach, A., Bertram, K., Hudecova, S., and Krizanova, O. (2015). Calcium and ROS: A mutual interplay. Redox Biol. 6, 260–271.

41. Schwartz, R.A., Carson, C.T., Schuberth, C., and Weitzman, M.D. (2009). Adeno-associated virus replication induces a DNA damage response coordinated by DNA-dependent protein kinase. J. Virol. 83, 6269–6278.

42. Bolderson, E., Scorah, J., Helleday, T., Smythe, C., and Meuth, M. (2004). ATM is required for the cellular response to thymidine induced replication fork stress. Hum. Mol. Genet. 13, 2937–2945.

43. Pei, X., Earley, L.F., He, Y., Chen, X., Hall, N.E., Samulski, R.J., and Li, C. (2018). Efficient capsid antigen presentation from adeno-associated virus empty virions in vivo. Front. Immunol. 9, 844.

44. Nass, S.A., Mattingly, M.A., Woodcock, D.A., Burnham, B.L., Ardinger, J.A., Osmond, S.E., Frederick, A.M., Scaria, A., Cheng, S.H., and O'Riordan, C.R. (2017). Universal Method for the Purification of Recombinant AAV Vectors of Differing Serotypes. Mol. Ther. Methods Clin. Dev. 9, 33–46.

45. Horowitz, E.D., Page, S., and Page, S. (2018). Biophysical and in Vitro Comparability Analysis of an Aav Vector Produced By the Baculovirus / Sf9 System and Hek Triple Transfection System. In ASGCT 23rd Annual Meeting, p. 5340.

46. Madigan, V.J., Yuziuk, J.A., Chiarella, A.M., Tyson, T.O., Meganck, R.M., Elmore, Z.C., Tse, L.V., Hathaway, N.A., and Asokan, A. (2019). Ring finger protein 121 is a potent regulator of adeno-associated viral genome transcription. PLoS Pathog. 15, e1007988.

47. Nayak, R., Farris, K.D., and Pintel, D.J. (2008). E4Orf6-E1B-55k-dependent degradation of de novo-generated adeno-associated virus type 5 Rep52 and capsid proteins employs a cullin 5-containing E3 ligase complex. J. Virol. 82, 3803–3808.

48. Zhong, L., Zhao, W., Wu, J., Li, B., Zolotukhin, S., Govindasamy, L., Agbandje-McKenna, M., and Srivastava, A. (2007). A dual role of EGFR protein tyrosine kinase signaling in ubiquitination of AAV2 capsids and viral second-strand DNA synthesis. Mol. Ther. 15, 1323–1330.

49. Koerber, J.T., Jang, J.H., and Schaffer, D.V. (2008). DNA shuffling of adeno-associated virus yields functionally diverse viral progeny. Mol. Ther. 16, 1703–1709.

50. Maheshri, N., Koerber, J.T., Kaspar, B.K., and Schaffer, D.V. (2006). Directed evolution of adeno-associated virus yields enhanced gene delivery vectors. Nat. Biotechnol. 24, 198–204.

51. Xiao, X., Li, J., and Samulski, R.J. (1998). Production of high-titer recombinant adeno-associated virus vectors in the absence of helper adenovirus. J. Virol. 72, 2224–2232.

52. Bardelli, M., Zarate-Perez, F., Agundez, L., Jolinon, N., Linden, R., Escalante, C., and Henckaerts, E. (2017). Analysis of Replicative Intermediates of Adeno-associated Virus through Hirt Extraction and Southern Blotting. Biol.-Protocol 7, e2271.